INVESTIGATION OF DARK CURRENT IN A S-DALINAC SUPERCONDUCTING CAVITY*

M. Gopych, H.-D. Gräf, U. Laier, M. Platz, A. Richter, A. Stascheck,
S. Wazlawik, Institut für Kernphysik, TU Darmstadt, Germany
S. Setzer, T. Weiland, TEMF, TU Darmstadt, Germany

Abstract

During the operation of the S-DALINAC [1], light emission associated with field emission on the surface from a 20 cell 3 GHz superconducting niobium rf cavity has been observed. The optical spectrum of the light spots has been measured by a photomultiplier using a set of filters. The obtained spectral density distribution is close to a black body radiation spectrum. In order to determine the maximum energy of the dark current electrons, measurements of bremsstrahlung spectra at the beam line exit of the accelerator have been carried out. For the interpretation of these data electron trajectory simulations based on field distributions calculated by MAFIA [2] have been performed. Additionally, the behavior of dark current has been investigated for different rf frequencies by means of numerical calculations for TESLA and S-DALINAC cavities.

INTRODUCTION

In this paper we present a detailed description of experiments on investigation of field emission accompanied by emission of light and results of simulations. The initial goal was to understand the reason for this phenomenon in a S-DALINAC cavity [1] means of extensive diagnostic measurements in oder to avoid this problem in the future. The measurements were performed downstream of the last superconducting cavity (#11) of the main linac. The design parameters of the cavity are summarized in Tab. 1. For the experiments the cavity remained installed in the accelerator cryostat, it was powered by a 500 W klystron and operated at a bath temperature of 2 K. Optical measurements were performed through the viewport in the straight beam line using a CCD camera, a monochromator, or a set of filters together with a photomultiplier. Bremsstrahlung spectra were taken with a BGO detector positioned directly above the beam line. According to preliminary experimental results reported in [3] the optical spectra measured using a spectrometer set up with high resolution was identified as a fluorescence spectrum of Cr^{3+} in chromium doped Al_2O_3. Further investigations have shown that the observed spectrum was due to scattered light from a fluorescence view screen behind the main linac. Although it was not positioned in the beam line during the measurements, the view screen was excited by dark current electrons from the cavity. Subsequently this target was replaced by a species fabricated from BeO and equipped with an improved shielding. In the following the determination of the maximum energy of dark current electrons via bremsstrahlung spectra is described, followed by an analysis of these results through extensive calculation of electron trajectories in the superconducting 20 cell cavity, using a combination of different numerical codes. Finally, the spectral distribution of the light, emitted from the bright spots inside the cavity, is presented and explained.

Table 1: Design parameters of the S–DALINAC accelerating structure

Material	Nb
Number of cells	20
Frequency	2.9975 GHz
Mode	π
Temperature	2 K
Quality Factor	$3{\cdot}10^9$
Accelerating Gradient	5 MV/m
RF Looses at 5 MV/M	4.2 W

BREMSSTRAHLUNG MEASUREMENTS

A significant part of field-emitted electrons is bent in the rf magnetic field and impacts on the cavity surface near the own emission site. But some electrons can be captured by the accelerating field and can traverse the entire cavity. The energy of these electrons can help to localize the cavity cell, where they started from. Bremsstrahlung produced by impacting electrons can be used to determine their maximum energy. It is the endpoint energy of the corresponding bremsstrahlung spectrum. The experimental set up is shown in Fig. 1. In oder to produce bremsstrahlung, the electrons, which were able to exit the cavity, are scattered from the view screen ((1) in Fig. 1) and hit the wall of the vacuum chamber. Bremsstrahlung spectra have been taken at accelerating gradients E_{acc} of 6.84, 6.66, 6.48 and 6.12 MV/m using a BGO detector ((2) in Fig. 1) located directly above the beam line. The values of the accelerating

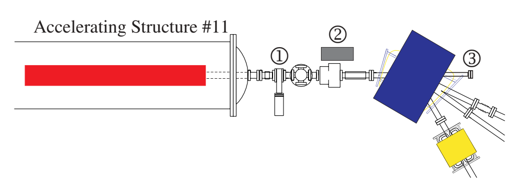

Figure 1: Experimental set up downstream of main linac. The figures denote: (1) view screen, (2) BGO detector, (3) viewport for optical measurements.

* Supported by the DFG (FOR 272/2-1 and GRK 410/2)

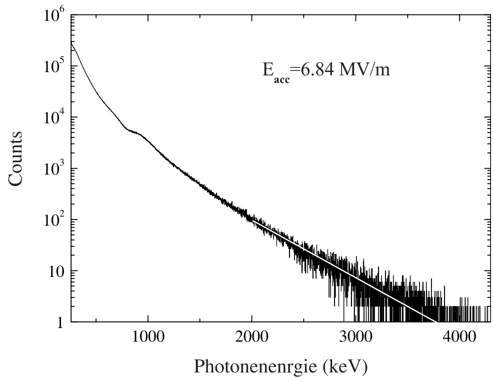

Figure 2: Bremsstrahlung spectrum taken with the BGO detector for E_{acc}=6.84 MV/m. The white line shows the exponential fit determining the endpoint energy.

gradients are known very accurately through calibrations from regular accelerator operation. As an example, the background corrected bremsstrahlung spectrum measured at $E_{acc} = 6.84$ MV/m is shown in Fig. 2. To evaluate the endpoint energy value an exponential fit has been used. For the spectrum in Fig. 2 the endpoint energy has been determined to 3.75 MeV. For other the spectra energies of 3.4, 3.05 and 2.3 MeV corresponding to decreasing accelerating gradients have been obtained. The experimental accuracy for the obtained energies is about 100 keV.

SIMULATION

In oder to explain the electron energies at the end of the cavity a simulation program for particle trajectories inside the cavity has been written. The trajectories of the field-emitted electrons in the accelerating structure are calculated numerically by integration of the relativistic equation of motion in electromagnetic fields using the Leap-Frog method. An initial field distribution in the accelerating structure was calculated using the MAFIA eigenmode solver [2] and used as an input file for the simulation code.

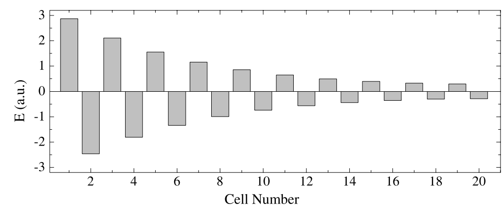

Figure 4: Field profile of a 20 cell S–DALINAC structure with the first cell detuned by 5 MHz

Because of the rotational symmetry of the considered cavity the simulation is performed in at r-z plane. The electron energy is saved for every integration step. Calculation of the trajectory is terminated when the electron hits the cavity wall. Space charge effects and the secondary emission process are not taken into account in the simulation program.

In a first attempt, a flat field distribution (i.e. field amplitude of the accelerating π-mode have equal magnitudes but opposite signs in neighboring cells) was assumed. Electrons were started with a zero velocity in a phase interval from -30° to 30° and scanning the entire region of an iris, where field emission occurs most likely. A time integration step of $5{\cdot}10^{-13}$ seconds was used to corresponding to 660 steps per rf period. An rf phase of 0° corresponds to the maximum electric field in the cell. These simulations have shown, that there were not any electrons which were able to gain an energy of more than 600 keV. The numerical calculations repeated for other irises provided the same result. Because the calculated energies did not agree with the experimental ones, similar simulations were performed for a TESLA cavity with an operating frequency of 1.3 GHz to check the correctness of the code. The numerical results for an accelerating gradient of 10 MV/m presented in [4] were exactly reproduced. Comparison between electron trajectories for TESLA and S–DALINAC cavities have shown that due to the higher frequency in the S–DALINAC considerably higher accelerating gradients are necessary to produce

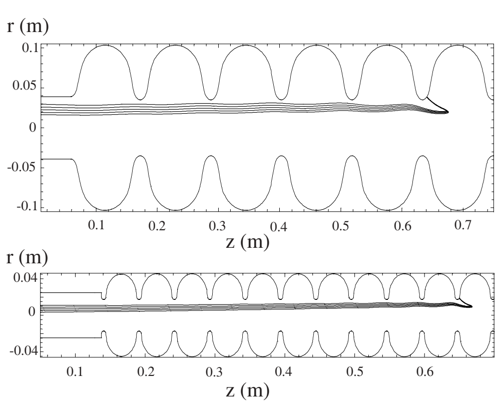

Figure 3: Electron trajectories in a TESLA (top) and in a S–DALINAC (bottom) structure for gradients of 10 and 23 MV/m respectively

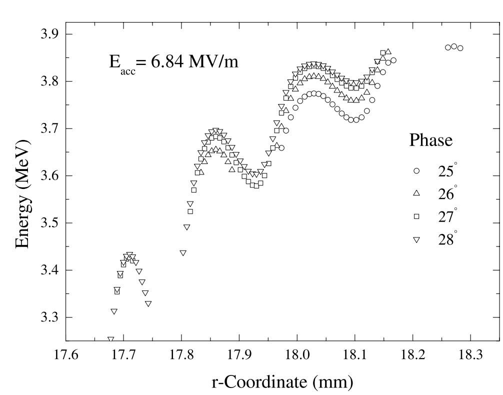

Figure 5: Energies of electrons at the end of the cavity as a function of the r coordinate of their start position on the iris for E_{acc}=6.84 MV/m.

similar trajectories to the ones in the TESLA cavity. The electrical field strengths must differ by a factor of 2.3 (the ratio of operating frequencies). Figure 3 shows electron trajectories in both cavities for gradients of 10 and 23 MV/m respectively. Remaining differences in the trajectories are attributed to the different cell shapes of the TESLA and S–DALINAC structure. Thus the assumption of a flat field profile had to be dropped in oder to explain the observed electron energies.

After initial fabrication all accelerating structures were tuned for flat field profiles. The operating π-mode, however, is extremely sensitive to perturbation of single cells (particularly the end cells) of multicell structures . As an example, a field profile of a 20 cell S–DALINAC structure with the first cell detuned by 5 MHz calculated from a simple lumped circuit model is shown in Fig. 4.

Table 2: Comparison of the energies obtained experimentally with the calculated ones .

E_{acc} (MV/m)	E_{kin} (MeV) Experiment	E_{kin} (MeV) Simulation
6.12	2.3 ± 0.1	2.16 ± 0.08
6.48	3.05 ± 0.1	3.1 ± 0.05
6.66	3.4 ± 0.1	3.45 ± 0.05
6.84	3.75 ± 0.1	3.8 ± 0.05

Under the assumption of such a field profile with the electron emission site located in a cell with high electric field it should be possible to explain the energies obtained from the bremsstrahlung spectra. Therefore the same simulations have been carried out for a cavity with a detuned first cell. Electrons started from the iris between the first and second cell because of the high electric field in this region. The field profile was obtained from the flat field distribution calculated with MAFIA scaled with the respective field amplitudes from cell to cell. Simulations for an accelerating structure with the first cell detuned by 5.4 MHz have succeeded in reproducing the experimental energies most suitably. Figure 5 shows energies of dark current electrons emerging from the cavity as a function of the r coordinate of their starting position on the iris between the first and second cell for accelerating gradient of 6.84 MV/m. The rounded part of the iris covers r coordinates from 17.325 to 20.525 mm. A comparison of experimentally observed and corresponding calculated energies is given in Tab. 2. The excellent agreement shows, that under the hypothesis of a detuned end cell (causing a non-flat field profile) the observed dark current energies can be explained.

OPTICAL MEASUREMENTS

After replacement of the chromium doped Al_2O_3 target the monochromator set up was no longer able to measure optical spectra due to lack of intensity, even though the

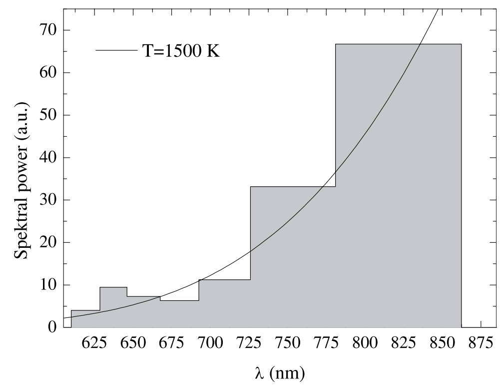

Figure 6: Spectrum of the light radiation emitted by the light spots.

bright, light emitting spots inside the cavity (reported earlier [3]) was clearly visible. Thus a set up of optical high-pass-filters, with cut-off-wavelengths ranging from 600-850 nm (in steps of 15 to 70 nm) together with a photomultiplier (Hamamatsu R1547) was used to determine the spectrum displayed in Fig. 6.

It shows increasing power starting at 600 nm toward the IR region. similar to a black body radiation spectrum. This result can be explained by a thermal model [5] according to a small particle thermally insulated from the surface of the cavity being heated by electric or magnetic field and loosing its energy by black body radiation. The curve giving in Fig. 6 for comparison shows the radiation power corresponding to a black body temperature of 1500 K.

The observation of light spots with a CCD camera placed at the exit of the accelerator has shown that all light spots were located in the second half of the cavity. On the other hand as shown by trajectory calculation, the sources of field emission must be located in the first cell of the cavity. This leads us to conclusion that the light spots are not associated with the field emission sites.

REFERENCES

[1] A. Richter, Proc. 5th Europ. Part. Acc. Conf., Eds. S. Myers, A. Pacheco, R. Pascual, Ch. Petit-Jean-Genaz and J. Poole, IOP Publisching, Bristol, (1996) 110.

[2] “MAFIA User Manual” CST-GmbH Büdinger Strasse 2a, D-64289 Darmstad.

[3] “Latest developments at the S–DALINAC” 8th Europ. Part. Acc. Conf. (2002) 2007.

[4] U. Becker, M. Zhang, T. Weiland “Two and Three Dimensional Simulations of Dark Current in TESLA-Cavities” 7th Workshop on RF-Superconductivity, Paris (1995) 397.

[5] W. Bauer, A. Citron, G. Dammertz, M. Grundner, L. Husson, H. Lengler, E. Rathgeber, IEEE Trans. NS-22 3 (1975) 1444.